

Published in final edited form as:

Free Radic Biol Med. 2014 August ; 0: 190–200. doi:10.1016/j.freeradbiomed.2014.05.006.

Hypothyroidism-associated missense mutation impairs NADPH oxidase activity and intracellular trafficking of Duox2

Ágnes Donkó^{1,2}, Stanislas Morand^{1,3}, Agnieszka Korzeniowska¹, Howard E. Boudreau¹, Melinda Zana², László Hunyady², Miklós Geiszt², and Thomas L. Leto^{1,*}

¹Laboratory of Host Defenses, National Institute of Allergy and Infectious Diseases, National Institutes of Health, Rockville, Maryland, USA

²Department of Physiology, Semmelweis University, Budapest, Hungary “Lendület” Peroxidase Enzyme Research Group of the Semmelweis University and the Hungarian Academy of Sciences, Budapest, Hungary

Abstract

In the thyroid gland Duox2-derived H₂O₂ is essential for thyroid hormone biosynthesis. Several patients were identified with partial or severe iodide organification defects caused by mutations in genes for Duox2 or its maturation factor, DuoxA2. A Duox2-deficient (*Duox2^{thyd}*) mouse model enabled *in vivo* investigation of its critical function in thyroid tissues, but its roles proposed in host defense or other innate responses in non-thyroid tissues remain less certain. These mice carry a spontaneous *DUOX2* missense mutation, a T>G transversion in exon 16 that changes the highly conserved valine 674 to glycine and results in severe congenital hypothyroidism. The exact mechanism underlying the effects of the V674G mutation has not been elucidated at the molecular or cellular level.

To determine how the V674G mutation leads to congenital hypothyroidism, we introduced the same mutation into human Duox2 or Duox1 cDNAs and expressed them in HEK-293 cells stably expressing the corresponding DuoxA proteins. We found the valine→glycine mutant Duox proteins fail to produce H₂O₂, lose their plasma membrane localization pattern and are retained within the endoplasmic reticulum. Duox2 mutant binds to DuoxA2, but appears to be unstable due to this retention. Immunohistochemical staining of Duox2 in murine salivary gland ducts showed Duox2 in mutant mice loses its condensed apical plasma membrane localization pattern characteristic of wild type Duox2 and accumulates in punctate vesicular structures within cells. Our findings demonstrate that changing the highly conserved valine 674 in Duox2 leads to impaired subcellular targeting and ROS release required for hormonogenesis, resulting in congenital hypothyroidism.

*corresponding author: Laboratory of Host Defenses, National Institute of Allergy and Infectious Diseases, National Institutes of Health, 12441 Parklawn Drive, Rockville, MD, 20852, USA. tleto@nih.gov.

³Current address: L'Oréal, Biotechnologies Department, Aulnay-Sous-Bois, France

Publisher's Disclaimer: This is a PDF file of an unedited manuscript that has been accepted for publication. As a service to our customers we are providing this early version of the manuscript. The manuscript will undergo copyediting, typesetting, and review of the resulting proof before it is published in its final citable form. Please note that during the production process errors may be discovered which could affect the content, and all legal disclaimers that apply to the journal pertain.

Keywords

Duox; mutation; hypothyroidism; NADPH oxidase

Introduction

Duox enzymes, Duox1 and Duox2, are members of the Nox family of NADPH oxidase enzymes that generate reactive oxygen species [1]. They were first both described in the thyroid gland, where they were proposed to be sources of hydrogen peroxide (H_2O_2) used by thyroid peroxidase for thyroid hormone biosynthesis [2, 3]. Congenital hypothyroidism is the most frequent inborn endocrine disorder and one of the most common preventable cause of mental retardation, with a prevalence of 1 in 3000-4000 newborns [4]. During the last decade several Duox2 mutations have been identified in a subset of patients with partial or total iodide organification defects resulting in transient to severe congenital hypothyroidism [5]. Duox maturation factors, a.k.a. Duox activators (DuoxA), are necessary for Duox to escape from the endoplasmic reticulum (ER) and undergo Golgi-based carbohydrate modifications, which are crucial steps in the formation of an active, H_2O_2 -generating Duox/DuoxA complex at the plasma membrane [6-8]. Two case studies with mild congenital hypothyroidism attributed to DuoxA2 mutations suggest some level of functional redundancy and compensation between the DuoxA1 and DuoxA2 maturation factors [9, 10]. Until now none of the reported congenital hypothyroid cases have been associated with mutations in the Duox1/DuoxA1 system [5], suggesting that Duox2/DuoxA2 is the primary H_2O_2 source supporting thyroid hormone biosynthesis [2]. This hypothesis is further supported by the fact that Duox1 knockout mice lack the congenital hypothyroid phenotype [11].

In non-thyroid tissues the Duox proteins are also thought to function primarily as extracellular H_2O_2 generators. Duox enzymes detected at high levels in exocrine glands (e.g. salivary) and on mucosal surfaces of gastrointestinal and airway epithelia were suggested to serve roles in antimicrobial host defense [12-14]. In the respiratory tract epithelium Duox accumulates on the apical plasma membrane, where a functional partnership was proposed with extracellular lactoperoxidase, which utilizes H_2O_2 to oxidize thiocyanate into an effective antimicrobial oxidant, hypothiocyanite [12, 15, 16]. In zebrafish and invertebrates, genetic evidence supports the role of Duox in gastrointestinal innate immunity [17-20], whereas in mammals the precise role of Duox enzymes in the gut epithelia is less certain and needs further study.

Consistent with the distinct expression patterns of the two Duox isoforms, their regulation shows tissue-specific characteristics [1, 21, 22]. While in human respiratory and intestinal epithelial cells Duox2 is upregulated by the Th1 cytokines, $IFN-\gamma$ and $TNF-\alpha$, [21, 23], in thyrocytes it is induced by the Th2 cytokines, IL-4 and IL-13 [22]. Furthermore, emerging evidence suggests that Duox2-derived H_2O_2 regulates innate immune responses by enhancing production of proinflammatory mediators that could stimulate adaptive immune responses [23-27]. Besides the beneficial proinflammatory effects of Duox2, it is becoming widely accepted that excessive ROS production can lead to pathologic cell functions.

According to this concept elevated Duox2 expression was found in patients with chronic pancreatitis, ulcerative colitis, Crohn's disease and in many human cancers [23, 26, 28]. In other systems, Duox enzymes also play an important role in extracellular matrix cross-linking [29, 30]; the produced H_2O_2 can serve as paracrine mediator in zebrafish [31], whereas in human lung epithelial cells ROS-based signals can accelerate cell migration [8, 32]. Many of these diverse functions involve extracellular release of H_2O_2 by Duox.

Duox-deficient mice represent unique experimental tools to examine the *in vivo* function of Duox2 in thyroid and other tissues; two Duox2-deficient mouse models have been described to date. Congenital hypothyroid mice with disruptions in both DuoxA maturation factor genes described recently lack functional forms of both Duox enzymes [33]. Another mouse strain (*Duox2^{thyd}*) that allows examination of critical Duox2 functions apart from DUOX1 carries a spontaneous *DUOX2* missense mutation (T>G base substitution in exon 16) that changes a highly conserved valine to glycine at residue 674 [34]. The V674G mutation results in a severe defect in thyroid hormone synthesis, manifested in congenital hypothyroidism with all the associated growth and developmental defects (dwarfism and hearing impairment). The V674G mutation is located between the first transmembrane helix and the calcium-binding EF-hand motifs of Duox2, within a region that was previously suggested to encompass an ER retention signal in the human Duox2 enzyme [35].

Since little is known at the molecular level about the interaction between Duox and their maturation factors and the exact mechanism underlying the effects of the V674G mutation has not been elucidated, the purpose of the current study was to explore in a heterologous expression system how the valine→glycine mutation leads to the loss of function and consequently to congenital hypothyroidism. We found that cells expressing the valine→glycine human Duox (hDuox) mutant enzymes failed to translocate Duox in the plasma membrane and release H_2O_2 . We show that valine→glycine Duox mutant enzymes are retained in the ER, where the V674G hDuox2 mutant remains in a complex with its Duox activator protein. Furthermore, the translocation defect of mutant Duox was verified in immunohistochemical studies of salivary gland sections from *Duox2^{thyd}* mice.

Materials and Methods

Animals

Duox2 mutant mice were purchased from The Jackson Laboratories. The recessive *thyd* mutation arose spontaneously in a B6(129)-Duox2^{thyd}/J mouse (Jackson Laboratory; Stock no. 005543), Duox1 knockout mice were purchased from Lexicon Genetics Inc. (The Woodlands, TX, USA) and were described in an earlier report [11]. Heterozygous mice were mated for simplified colony maintenance, since homozygous *thyd/thyd* mice suffer from severe hypothyroidism [34] (<http://jaxmice.jax.org/strain/005543.html>). Animal experiments were authorized by the Hungarian National Animal Experiment Committee under permission No. 22.1/1100/003/2008. Animals were maintained on a standard diet and given water *ad libitum*.

Genotyping of Duox2-mutant mice

Approximately 100 ng of purified tail genomic DNA was used as a template for PCR. To amplify the genomic 303-bp PCR product that contains the T→G change in exon 16, 5'-GAATCACATGGGCTCAAAGG-3' forward and 5'-ATGAAAACAGCCCCACAGAGG-3' reverse oligonucleotide primers were used with Taq LC polymerase (Fermentas, Ontario, Canada) according to the manufacturer's instructions. Cycling conditions were as follows: 94°C for 2 minutes, 38 cycles of 94°C 30 seconds, 58°C 30 seconds, 72°C 30 seconds and finally 72°C for 2 minutes. The PCR amplification yields a 303 bp product, which was digested with HaeIII at 37 °C for 1 hour and separated on 1.5 % agarose gels. The valine→glycine mutation creates an additional HaeIII cleavage site, resulting in further cleavage of the 226-bp HaeIII fragment into 166 bp and 60 bp bands. Genotyping of the Duox1 knockout mice was performed as described earlier [11].

cDNA and construction of mutations

The pcDNA5/FRT plasmids encoding the human tagged ^{HA}DUOX1 and ^{HA}DUOX2 cDNAs were previously characterized [7]. Mutations were prepared using the Quickchange II site-directed mutagenesis kit according to manufacturer's guidelines (Stratagene, La Jolla, CA, USA). After mutagenesis constructs were confirmed by DNA sequencing.

Cell culture and transfection of the cells

Flp-In 293 cell lines that stably express ^{V5h}DuoxA1α or ^{V5h}DuoxA2 were previously described by Morand, et al. [7]. Briefly, cells were cultured in minimum essential medium-α supplemented with 10% fetal bovine serum, 50 units/ml penicillin, 50 µg/ml streptomycin and 50 µg/ml hygromycin B (Life Technologies, Carlsbad, CA, USA) in a 5 % humidified CO₂ incubator at 37 °C. These lines were regularly assayed by Western blotting with anti-V5 to monitor DuoxA protein expression. Cells were transiently transfected with pcDNA5/FRT plasmid encoding human ^{HA}DUOX2, V674G/V674A/V674L/V674T ^{HA}DUOX2, ^{HA}DUOX1 or V670G ^{HA}DUOX1 cDNAs using the FuGene® 6 (Roche, Indianapolis, USA) or Lipofectamine® LTX with Plus™ (Life Technologies) transfection reagents according to the manufacturer's instructions. The cells were typically seeded in 6-well plates and transfected with 1-2 µg of plasmid DNA 24 hours later upon reaching densities of ~70% confluence. In some experiments transfection efficiencies were confirmed by including EGFP reporter plasmid (1:5 relative to Duox plasmid) or by determining plasmid-encoded Duox transcript copy numbers (relative to GAPDH) from reverse transcription/real time-PCR reactions by methods described earlier [36], using the SYBR Green PCR Mix (Invitrogen) and an ABI Prism 7500 RT-PCR System (Applied Biosystems/Life Technologies).

Measurement of H₂O₂ production

Two days after transfection cells were detached with Trypsin-EDTA, washed twice with HBSS buffer (Life Technologies) and counted in trypan blue solution (Lonza, Basel, Switzerland). Extracellular H₂O₂ production was measured in calcium and magnesium-containing HBSS in response to 1 µM ionomycin in the presence of 1 mM luminol and 20 U/ml horseradish peroxidase. Kinetic measurements of luminescence-based detection of

oxidized luminol were performed in 96-well white luminescence plates at 37 °C using 5×10^5 cells/well in a 200 μ l volume, monitored at 15 seconds intervals over a time course of 12 minutes in a Luminoskan luminometer (ThermoScientific, Waltham, MA, USA). Cells were stimulated with 1 μ M ionomycin. All measurements were carried out in triplicate. Data from multiple oxidase assays were normalized relative to 100% values observed with wild type Duox and were represented as means \pm standard errors of the mean. Differences between groups were analyzed by Kruskal-Wallis One Way Analysis of Variance on Ranks, using the Student-Newman-Keuls Method. P values less than 0.05 were considered as statistically significant.

Intracellular H_2O_2 was monitored by ratiometric FRET (Fluorescence resonance energy transfer) measurements using the cytosolic targeted PerFRET probe [37]. $V^5hDuoxA2$ expressing Flp-In 293 cells were seeded onto collagen coated glass coverslips and were cotransfected with PerFRET and wild -type or V674G H^ADuox2 encoding plasmids in a 1:4 ratio. Fluorescence intensity was detected on an inverted microscope (Axio Observer DL, Zeiss) equipped with a 40 \times 1.4 oil immersion objective (Fluar, Zeiss) and a Cascade II camera (Photometrics). The excitation wavelength of 435 nm was selected along with a Dual-View emission splitting system (505dcxr, 480/30 and 535/30; Photometrics) enabling the acquisition of simultaneous donor and raw FRET emissions. Excitation wavelengths were set by a random access monochromator connected to a xenon arc lamp (DeltaRAM, Photon Technology International). Images were acquired every 10 seconds for a period of 15 minutes. MetaFluor software (Molecular Devices) was used for programming and data analysis. Emission ratio was calculated after background fluorescence subtraction by dividing the raw FRET (Venus) and donor (Cerulean) emissions. Measurements were performed at 37°C in extracellular H-medium (145 mM NaCl, 5 mM KCl, 1 mM $MgCl_2$, 0.8 mM $CaCl_2$, 10 mM HEPES, 5 mM glucose, pH = 7.4).

Immunofluorescence, Confocal microscopy

Cells grown on collagen-coated 30 mm glass-bottom dishes (MatTek, Ashland, MA, USA) were fixed with 4% paraformaldehyde/PBS for 10 min, then permeabilized (or not) with 0.3% Triton X-100/PBS for 10 min and blocked with PBS supplemented with 5 % bovine serum albumin and 5 % normal goat serum at room temperature. Cells were then incubated with anti-HA (1:100; Covance), anti-V5 (1:200; Invitrogen) or anti-calnexin (1:50; Santa Cruz) for 2 hours at room temperature, and staining was revealed with Alexa Fluor® 594, 488 and 647 labeled secondary goat antibodies (1:1000) (LifeTechnologies). Nuclei were counterstained with DAPI (1:10000) (LifeTechnologies). Confocal fluorescence images were collected on a Leica SP2 confocal laser-scanning fluorescent microscope using a 63 \times oil immersion objective, NA 1.4 (Leica Microsystems, Wetzlar, Germany).

Flow cytometric analysis of cell-surface-exposed epitopes

Transfected cells (1×10^6) were detached using trypsin, blocked 15 min in 2 % FBS/PBS and sequentially incubated (30 min each) with anti-HA (1:100), anti-V5 (1:100), mouse IgG1 (1:10) or mouse IgG2a (1:25) isotype and mIgG1-Alexa⁶⁴⁷ or mIgG2a-Alexa⁴⁸⁸ (1:1000) secondary antibodies at 4 °C. After washing in ice cold PBS, fluorescence was monitored using a FACSort flow cytometer (BD Biosciences, San Jose, CA, USA). 10,000

events were acquired for each experiment and data analysis was performed with the WinMDI Version 2.8 software. For comparisons of several independent experiments, transfected cell populations exhibiting fluorescence intensities greater than the peak of DuoxA-expressing (non-transfected) cells were gated and plasma membrane exposure of the glycine mutants was normalized relative to the non-transfected cell peak and expressed as percent of the wild type Duox-transfected cells. V674G mutant Duox2 surface expression was analyzed by one-sample t-test and p values less than 0.05 were considered statistically significant.

Immunodetection of Duox2 in salivary gland

The polyclonal anti-Duox antibody was kindly provided by Dr. Xavier de Deken (Université Libre de Bruxelles). Frozen salivary gland sections from Duox1 knockout and Duox2-deficient mice were immunostained with this polyclonal anti-Duox antibody (raised against the Arg⁶¹⁸-His¹⁰⁴⁴ fragment of human Duox1) at a 1:150 dilution as previously described [11, 38].

Immunoblot analysis

Cell extracts (2×10^6) were prepared in cold NP-40 buffer (Boston Bioproducts, Ashland, MA, USA) supplemented with protease inhibitor cocktail (Sigma, St. Louis, MO, USA) by rocking on a rocker platform for 15 min at 4 °C and then cleared by centrifugation (10000 g, 10 min, 4 °C). Protein concentrations were determined by the BCA method (Pierce, Rockford, IL, USA). 50 µg of proteins were mixed with 4× LDS sample buffer (Life Technologies), loaded and separated by SDS-PAGE under reducing conditions, then transferred to nitrocellulose membranes (Life Technologies). Membranes were blocked in 1× TBS (Boston Bioproducts) with 5 % nonfat dry milk and 0.1% Tween 20 for 1 hour at room temperature and probed for 2 hours with anti-HA (1:2000; Covance), anti-HSP80 (1:2000; SantaCruz), anti-V5 (1:2000; Invitrogen) or anti-Duox (1:1000). Membranes were washed 6 times in TBS 0.1 % Tween 20 and incubated with HRP-conjugated goat antibodies for 1 hour (1:3000; GE Healthcare, Piscataway, NJ). Immune complexes were detected by chemiluminescence using an ECL Plus kit (GE Healthcare).

Immunoprecipitation assays

After 48 hours of transfection, 250-500 µg of cell lysates were incubated with 25-25 µl Pierce[®] Anti-HA-Agarose (ThermoScientific) or anti-V5-Agarose affinity gel (Sigma) for 1 hour at 4 °C on a rocking platform. After 3 washes with NP-40 buffer supplemented with protease inhibitor cocktail, bound proteins were eluted in DTT-containing 4× LDS buffer and subjected to SDS-PAGE followed by Western blot analysis.

Results

Mutation of the valine 674 to glycine impairs Duox H₂O₂ production

Valine 674 of murine Duox2 occurs at highly conserved position among different mammalian species, showing the same residue in Duox2 and Duox1 enzymes of rat, pig, dog and human [34]. In contrast, in zebrafish and nonvertebrate Duox isozymes this position is less conserved, being replaced by a threonine in mosquito, zebrafish, *Drosophila* and *C.*

C. elegans Duox2 or an alanine in *C. elegans* Duox1 (BLI-3). Since we previously established stable Flp-In 293 isogenic cell lines expressing single integrated copies of the human Duox maturation factors [7], we explored the effects of this valine→glycine mutation in the human Duox proteins. Attempts to establish stable mouse DuoxA2-expressing Flp-In 293 cells were not successful in reconstituting sufficient Duox2 oxidase activity when transfected with similar epitope-tagged versions of the murine proteins (data not shown). Using site-directed mutagenesis we replaced the valine 674 in human Duox2 and the corresponding valine 670 in human DUOX1 enzymes to glycine and transiently expressed them in clonally derived Flp-In 293 cells that stably express the human *DUOXA* maturation factor cDNAs. Since Duox enzymes produce H₂O₂ in response to a calcium signal, we stimulated cells with the calcium ionophore ionomycin and measured the ROS released into the extracellular space by chemiluminescence detecting luminol oxidation in the presence of HRP. While ionomycin stimulated a transient ROS production from wild type Duox2 (Figure 1A) and Duox1 (Figure 1B) enzymes, the valine→glycine mutant Duoxes failed to release extracellular H₂O₂.

Several mutant forms of hDuox2 associated with congenital hypothyroidism exhibit defects in translocation to the plasma membrane [5]. Therefore, we measured intracellular H₂O₂ production by Duox by independent means using the engineered ROS sensor protein PerFRET [37]. This probe undergoes conformational changes upon oxidation leading to decreased fluorescence emission through diminished intramolecular fluorescence resonance energy transfer. Our previous studies showed that a cytosolic-targeted version of this probe is capable of detecting ROS within cells expressing Duox, and can even detect ROS produced in neighboring Duox-expressing cells. DuoxA2-expressing Flp-In 293 cells were co-transfected with PerFRET and either wild type or mutant V674G^{HA}hDuox2. The Duox1-reconstituted model was not tested since these cells released significantly lower amounts of H₂O₂. As shown in Figure 1C, wild type Duox2-expressing cells exhibited decreased PerFRET fluorescence upon stimulation with ionomycin, which was further diminished by addition of extracellular H₂O₂. In contrast, V674G^{HA}hDuox2-transfected cells showed no decrease in PerFRET fluorescence upon stimulation with ionomycin.

To confirm that the inactive mutant Duox proteins are produced in these reconstituted cell models, we examined Duox protein expression in Western blot experiments. In spite of identical transfection conditions and protein lysates loaded to the gel, we always detected lower amounts of the valine→glycine Duox mutant proteins when compared with the wild type (Figure 2A), which shows that the mutant Duoxes have decreased protein stability or are produced less efficiently. In these experiments we used HA-tagged Duox and V5-tagged DuoxA proteins to circumvent any problems related to altered affinities or detection differences between mutant and wild type proteins with available Duox-specific antibodies, because we have shown previously that neither of these epitope tags affect enzyme activity, subcellular localization or Duox/DuoxA complex formation [7]. To confirm that the overall efficiencies of wild type and mutant Duox transfections were equivalent, we included EGFP plasmids (1:5 relative to the ^{HA}hDuox plasmid) in some experiments and saw no qualitative differences in overall transfection rates (not shown). Furthermore, we used real-time PCR assays of the reverse transcribed mRNAs from mutant and wild type Duox2-transfected cells

and saw no significant differences in the threshold cycle (Ct) detecting the mutant or wild type Duox2 transcripts in these cells. Together these findings suggest that the wild type and mutant ^{HA}hDuox plasmids are transfected and transcribed at equivalent levels, but that the valine→glycine mutant proteins are rendered inactive in comparison to wild type proteins.

To explore the effects of the V674G Duox mutation further, we created other mutations at this site: alanine and threonine substitutions were modeled from Duox sequence in lower species, whereas a leucine substitution was based on its similarity to valine. ^{V5}hDuoxA2 expressing cells transiently transfected with the V674T and V674L ^{HA}hDuox2 produced protein at levels comparable to wild type ^{HA}hDuox2, whereas the V674A ^{HA}hDuox2 protein was observed by blotting at considerably lower levels, detected with anti-HA and anti-Duox antibodies (Figure 2B). As expected, the V674A ^{HA}hDuox2-expressing cells exhibited undetectable ROS production in response to ionomycin, whereas V674T and V674L ^{HA}hDuox2 transfected cells produced ROS at levels that matched or exceeded that of wild type ^{HA}hDuox2-expressing cells (Fig 2C). These finding revealed a strong requirement for bulky aliphatic amino acid side chains at Duox2 position 674, as both the Gly and Ala mutant proteins appeared to be considerably less stable.

The valine→glycine mutant Duox enzymes are not targeted to the plasma membrane

The extracellular N-terminal HA and V5 epitope tags on Duox and DuoxA proteins enabled us to investigate cell surface exposure of both proteins in intact cells by flow cytometry. While the wild type ^{HA}hDuox2 is transported and expressed on the plasma membrane along with the ^{V5}hDuoxA2 maturation factor in unpermeabilized fixed cells, the valine 674 mutant enzyme was not detected on the cell surface in unpermeabilized cells (Figure 3A); similar results were observed when the ^{V5}hDuoxA2 was expressed alone (Figure 3B). We obtained identical results with V670G ^{HA}hDuox1 mutant expressed in stable ^{V5}hDuoxA1α Flp-In cells (Figure 3C, 3D). To compare the WT and mutant Duox proteins, we gated for the transfected cell population and expressed surface exposure of the glycine mutants as percent of the wild type Duox plasma membrane expression. Analysis of 3 independent Duox2 transfections (Figure 3E) revealed a significant difference in relative plasma membrane expression between WT and Gly mutant expressing cells.

To confirm and extend these flow cytometry observations on cell surface targeting, we also performed immunofluorescence imaging of staining of Flp-In 293 cells that stably express ^{V5}hDuox activators and were transiently transfected with wild type or mutant ^{HA}hDuox2 and ^{HA}hDUOX1 enzymes. Since both the HA and the V5 tagged portions of the proteins are located within extracellular domains, we examined cell surface expression on unpermeabilized cells. While the ^{HA}hDuox1 and ^{HA}hDuox2 wild type proteins clearly colocalize with activators on the cell surface, neither valine→glycine ^{HA}hDuox mutant enzyme nor their corresponding ^{V5}hDuoxA maturation factors were detected on the plasma membrane in unpermeabilized cells (Figure 4).

The valine→glycine mutant Duox enzymes are retained in the endoplasmic reticulum

Several studies indicate that heterologously expressed Duox enzymes do not reach the cell surface but are retained in the ER in absence of their corresponding DuoxA maturation

factors [6, 9, 39, 40]. To determine where the valine→glycine ^{HA}hDuox1 and ^{HA}hDuox2 mutants are located inside the cells we performed immunofluorescence staining on permeabilized Flp-In 293 along with staining for the ER marker chaperon protein, calnexin. In the cases of wild type ^{HA}hDuox enzymes the majority of the proteins are located on the plasma membrane along with the activators, but in contrast to wild type enzymes, the V674G ^{HA}hDuox2 and V670G ^{HA}hDuox1 mutants are retained inside the cells, where they colocalize with their activator proteins along with the ER marker calnexin (Figure 5).

The valine→glycine hDuox1 mutant forms a stable complex with DuoxA2

Previously it was shown that Duox2 forms a stable complex with DuoxA2 that can be precipitated from the cell surface, but not when expressed with mismatched DuoxA1α or DuoxA1γ isoforms [7]. Because little is known at the molecular level about the amino acid residues determining the interaction between Duox and DuoxA proteins, we investigated the effect of the valine 674 to glycine mutation on Duox-DuoxA complex formation in immunoprecipitation experiments. Stable ^{V5}hDuoxA2 expressing Flp-In 293 cells were transiently transfected with wild type or V674G ^{HA}hDuox2 mutant enzyme and after 48 hours cells were lysed and incubated with anti-HA or anti-V5 agarose. Western blot analysis detected stable Duox2-DuoxA2 complexes even in the case of valine→glycine Duox2 mutant in both HA- and V5-agarose precipitation experiments, although lower quantities of both proteins were captured in these precipitated complexes (Figure 6).

Detection of endogenous V674G Duox2 mutant in salivary glands

To detect the endogenous valine→glycine mutant Duox2 protein, we performed immunohistochemistry on salivary gland sections from the hypothyroid Duox2^{hyd} mutant mice. Earlier studies showed that Duox2 expression is particularly high in salivary ductal epithelial cells [12], whereas expression of both Duox isoforms is detected in thyroid tissue. Because the Duox antibody we used in this study does not discriminate between the two Duox isoforms, we examined Duox1 knockout mouse tissues as a reference, where, in the absence of Duox1, we detect solely the Duox2 protein. In the Duox1 knockout salivary gland sections, the wild type Duox2 is detected in a condensed staining pattern along the apical aspect of ductal epithelial cells, whereas in the V674G mutant salivary gland sections, the Duox2 staining is less intense along apical plasma membrane and the protein appears to form dot-like vesicular structures within intracellular sites (Figure 7).

Discussion

Investigators on the thyroid metabolism field have long appreciated that this tissue has a high capacity for oxidant production required for iodine oxidation and for thyroglobulin iodination during thyroid hormone biosynthesis. Well before all the components involved in this process were identified, early radioiodination studies revealed that these oxidative processes are tightly regulated and confined to the thyroid follicle lumen (thyrocyte apical surface) in order to prevent toxic ROS generation within the cell [41, 42]. The Duox2-DuoxA2 system was later identified as an indispensable source of extracellular H₂O₂ in the thyroid gland, as mutations of either Duox2 or DuoxA2 were shown to cause hypothyroidism due to insufficient H₂O₂ generation required to support thyroperoxidase-

mediated thyroid hormone biosynthesis (reviewed in [5]). A spontaneously occurring point mutation of valine 647 in murine Duox2 results in severe congenital hypothyroidism in homozygous *thyd/thyd* mice, suggesting an essential role for this conserved amino acid in extracellular ROS production [34]. The *thyd/thyd* mice grow to only one-half the size of control littermates, have approximately one-ten and one-twentieth of normal circulating levels of thyroxine and insulin-like growth factor-1, respectively, and 100-1000× the normal levels of thyroid-stimulating hormone levels. As a consequence of the reduced thyroid hormone levels the homozygous mutant mice develop short bones with diminished bone mineral density and defects in the inner ear development resulting in hearing loss typical of severe congenital hypothyroidism. To explore the consequences of this mutation we have introduced the valine 674 to glycine mutation into human Duox2, as well as the corresponding valine 670 mutation into human Duox1. We found that in the heterologous expression systems both valine→glycine human Duox mutant enzymes failed to release extracellular H₂O₂ in response to intracellular calcium signals (Figure 1). Valine 674 is located in the first intracellular loop that exhibits no homology to other known protein domains, between the first transmembrane helix (res. 596-620) and the calcium ion binding EF-hand motifs (res. 832-843). In this region the first heterozygous mutations: Q686X and R701X were reported to cause premature termination signals that were associated with mild and transient hypothyroidism at early stages of life when the demand for thyroid hormone is the greatest [43]. Two other Duox2 biallelic missense mutations in this region, A649E and H678R, were suggested to cause transient congenital hypothyroidism, but these amino acid changes were associated with additional mutations (R885Q and L1067S, respectively) and their effects on the ROS production have not been elucidated [44]. Later it was shown that the H678R Duox2 polymorphism, close to the murine Duox2 mutation we studied, exhibits normal cell surface expression and only slight decreases in H₂O₂ producing activity [45, 46]. Several other hDuox2 missense mutations reviewed recently [5] were shown to affect translocation of Duox to the plasma membrane (*i.e.*, the extracellular peroxidase homology domain mutations: Q36H, R376W, D506N), although the effects of the murine V674G Duox2 mutation appears to reflect distinct local structural requirements affecting protein stability as well subcellular targeting.

We determined that the mutation of the valine 674 of hDuox2 or the homologous valine 670 mutation of hDuox1 affect intracellular trafficking, such that the extracellular epitope-tagged mutant Duox enzymes could not be detected at the cell surface either by flow cytometry or by immunofluorescence staining of unpermeabilized cells (Figure 3 and 4). It has been shown that only glycosylated and completely processed Duox enzymes are transported to the plasma membrane and produce H₂O₂, while the partially processed forms of glycosylated Duox proteins are retained in the endoplasmic reticulum [6, 9, 39, 40]. Until the discovery of Duox maturation factors (DuoxA1 and DuoxA2) expression of active Duox enzymes was not possible. The Duox activators were originally described as ER resident maturation factors that allowed Duox to escape the ER and reconstitute full enzymatic activity [6]. Later the DuoxA proteins were shown to form stable complexes with Duox proteins that are processed and co-translocated to the plasma membrane as part of the active ROS-generating complexes [7, 8]. Immunofluorescent staining of permeabilized cells indicated that the valine→glycine Duox mutant enzymes are retained within the

endoplasmic reticulum colocalized with Duox activators and the ER specific calnexin protein (Figure 5). The translocation defect of valine 674 Duox2 mutant was verified by immunohistochemical staining of salivary gland sections from the Duox2^{thyd} mutant mice, where mutant Duox2 was detected at considerably lower levels than native, wild type Duox2 and was less condensed along the luminal plasma membrane of major duct epithelial cells, while forming punctate or vesicular structures within cells (Figure 7).

In order to better understand structural requirements of position 674 and the effects of the V674G mutation on protein stability and subcellular targeting, we investigated several other Duox2 mutations. Valine 674 was converted to alanine, threonine or leucine. While alanine (CeDuox1) and threonine (mosquito, zebrafish, CeDuox) substitutions are observed in Duox in lower species, the leucine mutant was created as another residue bearing a bulky hydrophobic side-chain similar to the highly conserved valine.

Studies of these new residue 674 mutations on Duox2 activity and expression (Figure 2B, C) revealed that there is a structural requirement for bulky, uncharged residues at this site, since leucine and threonine mutants are fully active, whereas the alanine substitution (small side chain similar to glycine) renders Duox2 inactive and unstable, consistent with disruptive effects of the spontaneous glycine mutation. Structural predictions deduced through analysis by Chou-Fasman, GOR, and neural network algorithms (<http://cib.cf.ocha.ac.jp/bitool/MIX/>) all suggest that the segment from residues 672-678 of the native protein is folded in an alpha-helical conformation, whereas the substitution of glycine 674, a known disrupter of alpha-helical structure, drastically reduces the probability of alpha-helical structure throughout this segment. Our observations strongly suggest that misfolding of this region perturbs interactions or induces aggregation, thereby resulting in an inefficient exit of the Duox/DuoxA complex from the ER.

In our transfected Flp-In 293 cell system, coimmunoprecipitation of the transiently transfected valine→glycine hDuox2 mutant enzyme detected a complex with DuoxA2 within the ER (Figures 5). Analysis of the protein produced suggested that the valine→glycine hDuox2 mutant is intrinsically less stable than wild type; this was even more pronounced with the valine→glycine hDuox1 mutant protein (Figure 2), which precluded coimmunoprecipitation experiments with the mutant hDuox1 protein.

In summary, we characterized the effects of a spontaneously generated valine 674 to glycine mutation of murine Duox2 in a heterologous expression system using the human Duox proteins, and we concluded that this substitution results in a translocation defect and complete loss of function that explains the severe congenital hypothyroid phenotype of the *thyd/thyd* mouse strain (Figure 8). While the instability and defective targeting of mutant Duox2 was confirmed in salivary glands of *thyd/thyd* mice, this animal model poses serious limitations for studies of Duox2 function in non-thyroid tissues because of the profound overriding defects in growth and development associated with the severe hypothyroidism phenotype in these animals related to low circulating thyroid hormone and IGF-1 levels. Experiments designed to correct thyroid hormone insufficiency in this model should be considered cautiously, since even minor hyperthyroidism or hypothyroidism could affect development, adaptive and innate immunity, and inflammatory processes in many tissues

[44]. Therefore, strategies aimed at inducible, tissue-specific knockout of Duox2 expression would be ideally suited for investigations of Duox2 functions in non-thyroid tissues.

Acknowledgments

We are grateful to Beáta Molnár and Tiinde Szosznyák for technical assistance. We thank Dr. László Szidonya for critical reading of the manuscript and Dr. Xavier de Deken for generously providing the anti-Duox antibody. This work was supported by grants from the Hungarian Research Fund (OTKA PD103960, OTKA K106138) and the Hungarian Academy of Sciences ("Lendület" Programme) and funds from the Intramural Research Program of the NIH, National Institute of Allergy and Infectious Diseases.

References

1. Donko A, Peterfi Z, Sum A, Leto T, Geiszt M. Dual oxidases. Philosophical transactions of the Royal Society of London Series B, Biological sciences. 2005; 360:2301–2308.
2. Dupuy C, Ohayon R, Valent A, Noel-Hudson MS, Deme D, Virion A. Purification of a novel flavoprotein involved in the thyroid NADPH oxidase. Cloning of the porcine and human cdnas. J Biol Chem. 1999; 274:37265–37269. [PubMed: 10601291]
3. De DX, Wang D, Many MC, Costagliola S, Libert F, Vassart G, Dumont JE, Miot F. Cloning of two human thyroid cDNAs encoding new members of the NADPH oxidase family. J Biol Chem. 2000; 275:23227–23233. [PubMed: 10806195]
4. Rose SR, Brown RS, Foley T, Kaplowitz PB, Kaye CI, Sundararajan S, Varma SK. Update of newborn screening and therapy for congenital hypothyroidism. Pediatrics. 2006; 117:2290–2303. [PubMed: 16740880]
5. Grasberger H. Defects of thyroidal hydrogen peroxide generation in congenital hypothyroidism. Molecular and cellular endocrinology. 2010; 322:99–106. [PubMed: 20122987]
6. Grasberger H, Refetoff S. Identification of the maturation factor for dual oxidase. Evolution of an eukaryotic operon equivalent. The Journal of biological chemistry. 2006; 281:18269–18272. [PubMed: 16651268]
7. Morand S, Ueyama T, Tsujibe S, Saito N, Korzeniowska A, Leto TL. Duox maturation factors form cell surface complexes with Duox affecting the specificity of reactive oxygen species generation. FASEB journal : official publication of the Federation of American Societies for Experimental Biology. 2009; 23:1205–1218. [PubMed: 19074510]
8. Luxen S, Noack D, Frausto M, Davanture S, Torbett BE, Knaus UG. Heterodimerization controls localization of Duox-DuoxA NADPH oxidases in airway cells. Journal of cell science. 2009; 122:1238–1247. [PubMed: 19339556]
9. Zamproni I, Grasberger H, Cortinovis F, Vigone MC, Chiumello G, Mora S, Onigata K, Fugazzola L, Refetoff S, Persani L, Weber G. Biallelic inactivation of the dual oxidase maturation factor 2 (DUOXA2) gene as a novel cause of congenital hypothyroidism. The Journal of clinical endocrinology and metabolism. 2008; 93:605–610. [PubMed: 18042646]
10. Hulur I, Hermanns P, Nestoris C, Heger S, Refetoff S, Pohlenz J, Grasberger H. A single copy of the recently identified dual oxidase maturation factor (DUOXA) 1 gene produces only mild transient hypothyroidism in a patient with a novel biallelic DUOXA2 mutation and monoallelic DUOXA1 deletion. The Journal of clinical endocrinology and metabolism. 2011; 96:E841–845. [PubMed: 21367925]
11. Donko A, Ruisanchez E, Orient A, Enyedi B, Kapui R, Peterfi Z, de Deken X, Benyo Z, Geiszt M. Urothelial cells produce hydrogen peroxide through the activation of Duox1. Free radical biology & medicine. 2010; 49:2040–2048. [PubMed: 21146788]
12. Geiszt M, Witta J, Baffi J, Lekstrom K, Leto TL. Dual oxidases represent novel hydrogen peroxide sources supporting mucosal surface host defense. FASEB J. 2003; 17:1502–1504. [PubMed: 12824283]
13. El Hassani RA, Benfares N, Caillou B, Talbot M, Sabourin JC, Belotte V, Morand S, Gnidehou S, Agnandji D, Ohayon R, Kaniewski J, Noel-Hudson MS, Bidart JM, Schlumberger M, Virion A, Dupuy C. Dual oxidase2 is expressed all along the digestive tract. Am J Physiol Gastrointest Liver Physiol. 2005; 288:G933–G942. [PubMed: 15591162]

14. Allaoui A, Botteaux A, Dumont JE, Hoste C, De Deken X. Dual oxidases and hydrogen peroxide in a complex dialogue between host mucosae and bacteria. *Trends in molecular medicine*. 2009; 15:571–579. [PubMed: 19913458]
15. Forteza R, Salathe M, Miot F, Conner GE. Regulated hydrogen peroxide production by Duox in human airway epithelial cells. *Am J Respir Cell Mol Biol*. 2005; 32:462–469. [PubMed: 15677770]
16. Moskwa P, Lorentzen D, Excoffon KJ, Zabner J, McCray PB Jr, Nauseef WM, Dupuy C, Banfi B. A novel host defense system of airways is defective in cystic fibrosis. *American journal of respiratory and critical care medicine*. 2007; 175:174–183. [PubMed: 17082494]
17. Ha EM, Lee KA, Park SH, Kim SH, Nam HJ, Lee HY, Kang D, Lee WJ. Regulation of DUOX by the Galphaq-phospholipase C β -Ca $^{2+}$ pathway in *Drosophila* gut immunity. *Developmental cell*. 2009; 16:386–397. [PubMed: 19289084]
18. Flores MV, Crawford KC, Pullin LM, Hall CJ, Crosier KE, Crosier PS. Dual oxidase in the intestinal epithelium of zebrafish larvae has anti-bacterial properties. *Biochemical and biophysical research communications*. 2010; 400:164–168. [PubMed: 20709024]
19. Chavez V, Mohri-Shiomi A, Garsin DA. Ce-Duox1/BLI-3 generates reactive oxygen species as a protective innate immune mechanism in *Caenorhabditis elegans*. *Infection and immunity*. 2009; 77:4983–4989. [PubMed: 19687201]
20. Hoeven R, McCallum KC, Cruz MR, Garsin DA. Ce-Duox1/BLI-3 generated reactive oxygen species trigger protective SKN-1 activity via p38 MAPK signaling during infection in *C. elegans*. *PLoS pathogens*. 2011; 7:e1002453. [PubMed: 22216003]
21. Harper RW, Xu C, Eiserich JP, Chen Y, Kao CY, Thai P, Setiadi H, Wu R. Differential regulation of dual NADPH oxidases/peroxidases, Duox1 and Duox2, by Th1 and Th2 cytokines in respiratory tract epithelium. *FEBS letters*. 2005; 579:4911–4917. [PubMed: 16111680]
22. Raad H, Eskalli Z, Corvilain B, Miot F, De Deken X. Thyroid hydrogen peroxide production is enhanced by the Th2 cytokines, IL-4 and IL-13, through increased expression of the dual oxidase 2 and its maturation factor DUOXA2. *Free radical biology & medicine*. 2013; 56:216–225. [PubMed: 23010498]
23. Lipinski S, Till A, Sina C, Arlt A, Grasberger H, Schreiber S, Rosenstiel P. DUOX2-derived reactive oxygen species are effectors of NOD2-mediated antibacterial responses. *Journal of cell science*. 2009; 122:3522–3530. [PubMed: 19759286]
24. Joo JH, Ryu JH, Kim CH, Kim HJ, Suh MS, Kim JO, Chung SY, Lee SN, Kim HM, Bae YS, Yoon JH. Dual oxidase 2 is essential for the toll-like receptor 5-mediated inflammatory response in airway mucosa. *Antioxidants & redox signaling*. 2012; 16:57–70. [PubMed: 21714724]
25. Yu H, Zhou X, Wen S, Xiao Q. Flagellin/TLR5 responses induce mucus hypersecretion by activating EGFR via an epithelial cell signaling cascades. *Experimental cell research*. 2012; 318:723–731. [PubMed: 22227411]
26. Wu, Y.; Lu, J.; Antony, S.; Juhasz, A.; Liu, H.; Jiang, G.; Meitzler, JL.; Hollingshead, M.; Haines, DC.; Butcher, D.; Roy, K.; Doroshov, JH. *Journal of immunology*. Vol. 190. Baltimore, Md.: 2013. Activation of TLR4 is required for the synergistic induction of dual oxidase 2 and dual oxidase A2 by IFN- γ and lipopolysaccharide in human pancreatic cancer cell lines; p. 1859-1872.1950
27. Yu, M.; Lam, J.; Rada, B.; Leto, TL.; Levine, SJ. *Journal of immunology*. Vol. 186. Baltimore, Md.: 2011. Double-stranded RNA induces shedding of the 34-kDa soluble TNFR1 from human airway epithelial cells via TLR3-TRIF-RIP1-dependent signaling: roles for dual oxidase 2- and caspase-dependent pathways; p. 1180-1188.1950
28. Wu Y, Antony S, Hewitt SM, Jiang G, Yang SX, Meitzler JL, Juhasz A, Lu J, Liu H, Doroshov JH, Roy K. Functional activity and tumor-specific expression of dual oxidase 2 in pancreatic cancer cells and human malignancies characterized with a novel monoclonal antibody. *International journal of oncology*. 2013; 42:1229–1238. [PubMed: 23404210]
29. Anh NT, Nishitani M, Harada S, Yamaguchi M, Kamei K. Essential role of Duox in stabilization of *Drosophila* wing. *The Journal of biological chemistry*. 2011; 286:33244–33251. [PubMed: 21808060]

30. Edens WA, Sharling L, Cheng G, Shapira R, Kinkade JM, Lee T, Edens HA, Tang X, Sullards C, Flaherty DB, Benian GM, Lambeth JD. Tyrosine cross-linking of extracellular matrix is catalyzed by Duox, a multidomain oxidase/oxidoreductase with homology to the phagocyte oxidase subunit gp91phox. *J Cell Biol.* 2001; 154:879–891. [PubMed: 11514595]
31. Niethammer P, Grabher C, Look AT, Mitchison TJ. A tissue-scale gradient of hydrogen peroxide mediates rapid wound detection in zebrafish. *Nature.* 2009; 459:996–999. [PubMed: 19494811]
32. Gorissen SH, Hristova M, Habibovic A, Sipsey LM, Spiess PC, Janssen-Heininger YM, van der Vliet A. Dual oxidase-1 is required for airway epithelial cell migration and bronchiolar reepithelialization after injury. *American journal of respiratory cell and molecular biology.* 2013; 48:337–345. [PubMed: 23239498]
33. Grasberger, H.; De Deken, X.; Mayo, OB.; Raad, H.; Weiss, M.; Liao, XH.; Refetoff, S. *Molecular endocrinology.* Vol. 26. Baltimore, Md.: 2012. Mice deficient in dual oxidase maturation factors are severely hypothyroid; p. 481–492.
34. Johnson, KR.; Marden, CC.; Ward-Bailey, P.; Gagnon, LH.; Bronson, RT.; Donahue, LR. *Molecular endocrinology.* Vol. 21. Baltimore, Md.: 2007. Congenital hypothyroidism, dwarfism, and hearing impairment caused by a missense mutation in the mouse dual oxidase 2 gene, Duox2; p. 1593–1602.
35. Morand S, Agnandji D, Noel-Hudson MS, Nicolas V, Buisson S, Macon-Lemaitre L, Gnidehou S, Kaniewski J, Ohayon R, Virion A, Dupuy C. Targeting of the dual oxidase 2 N-terminal region to the plasma membrane. *J Biol Chem.* 2004; 279:30244–30251. [PubMed: 15150274]
36. Rada B, Boudreau HE, Park JJ, Leto TL. Histamine Stimulates Hydrogen Peroxide Production by Bronchial Epithelial Cells via Histamine H1 Receptor and Duox. *American journal of respiratory cell and molecular biology.* 2013
37. Enyedi B, Zana M, Donko A, Geiszt M. Spatial and Temporal Analysis of NADPH Oxidase-Generated Hydrogen Peroxide Signals by Novel Fluorescent Reporter Proteins. *Antioxidants & redox signaling.* 2012
38. Milenkovic M, De Deken X, Jin L, De Felice M, Di Lauro R, Dumont JE, Corvilain B, Miot F. Duox expression and related H₂O₂ measurement in mouse thyroid: onset in embryonic development and regulation by TSH in adult. *The Journal of endocrinology.* 2007; 192:615–626. [PubMed: 17332529]
39. Ameziane-El-Hassani R, Morand S, Boucher JL, Frapart YM, Apostolou D, Agnandji D, Gnidehou S, Ohayon R, Noel-Hudson MS, Francon J, Lalaoui K, Virion A, Dupuy C. Dual oxidase-2 has an intrinsic Ca²⁺-dependent H₂O₂-generating activity. *The Journal of biological chemistry.* 2005; 280:30046–30054. [PubMed: 15972824]
40. Grasberger, H.; De Deken, X.; Miot, F.; Pohlenz, J.; Refetoff, S. *Molecular endocrinology.* Vol. 21. Baltimore, Md.: 2007. Missense mutations of dual oxidase 2 (DUOX2) implicated in congenital hypothyroidism have impaired trafficking in cells reconstituted with DUOX2 maturation factor; p. 1408–1421.
41. Bjorkman U, Ekholm R, Denef JF. Cytochemical localization of hydrogen peroxide in isolated thyroid follicles. *Journal of ultrastructure research.* 1981; 74:105–115. [PubMed: 6264094]
42. Ekholm R. Iodination of thyroglobulin. An intracellular or extracellular process? *Molecular and cellular endocrinology.* 1981; 24:141–163. [PubMed: 7028537]
43. Moreno JC, Bikker H, Kempers MJ, van Trotsenburg AS, Baas F, de Vijlder JJ, Vulsma T, Ris-Stalpers C. Inactivating mutations in the gene for thyroid oxidase 2 (THOX2) and congenital hypothyroidism. *N Engl J Med.* 2002; 347:95–102. [PubMed: 12110737]
44. Maruo Y, Takahashi H, Soeda I, Nishikura N, Matsui K, Ota Y, Mimura Y, Mori A, Sato H, Takeuchi Y. Transient congenital hypothyroidism caused by biallelic mutations of the dual oxidase 2 gene in Japanese patients detected by a neonatal screening program. *The Journal of clinical endocrinology and metabolism.* 2008; 93:4261–4267. [PubMed: 18765513]
45. De Marco G, Agretti P, Montanelli L, Di Cosmo C, Bagattini B, De Servi M, Ferrarini E, Dimida A, Freitas Ferreira AC, Molinaro A, Ceccarelli C, Brozzi F, Pinchera A, Vitti P, Tonacchera M. Identification and functional analysis of novel dual oxidase 2 (DUOX2) mutations in children with congenital or subclinical hypothyroidism. *The Journal of clinical endocrinology and metabolism.* 2011; 96:E1335–1339. [PubMed: 21565790]

46. Narumi S, Muroya K, Asakura Y, Aachi M, Hasegawa T. Molecular basis of thyroid dysmorphogenesis: genetic screening in population-based Japanese patients. *The Journal of clinical endocrinology and metabolism*. 2011; 96:E1838–1842. [PubMed: 21900383]

Highlights

- We explored effects of the *Duox2^{thyd}* mutation causing hypothyroidism in mice.
- V674G Duox2 and V670G Duox1 failed to produce extracellular hydrogen peroxide.
- Mutant Duox forms a complex with its maturation factor but is retained in the ER
- Staining of salivary glands from *thyd* mice verified the Duox2 translocation defect.

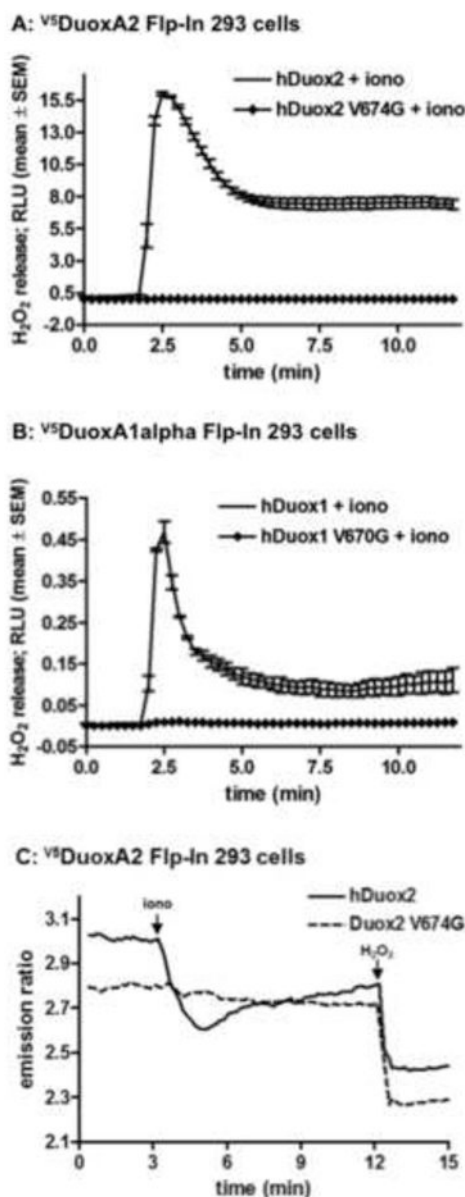


Figure 1. Measurement of H_2O_2 release of the valine→glycine mutant Duox enzymes
 (A, B) Stable V^5 hDuoxA-expressing Flp-In 293 cell lines transiently transfected with wild type or mutant V674G HA hDUOX2 or V670G HA hDUOX1 cDNAs were stimulated with 1 μ M ionomycin. Data collected from triplicate measurements in a luminescence plate reader are shown from one representative assay from at least three independent experiments. Error bars reflect mean \pm standard error of the mean.
 (C) Fluorescence emission ratio (535/480nm) of V^5 hDuoxA-Flp-In 293 cells co-expressing the cytosol targeted H_2O_2 sensor, PerFRET, and wild type or mutant V674G HA hDuox2 proteins. After acquisition of a baseline emission, H_2O_2 production was stimulated with 1 μ M ionomycin (iono) and then the probe was maximally oxidized by the addition of 100 μ M H_2O_2 . Curves represents the average from 2 independent experiments, n=40-50 cells.

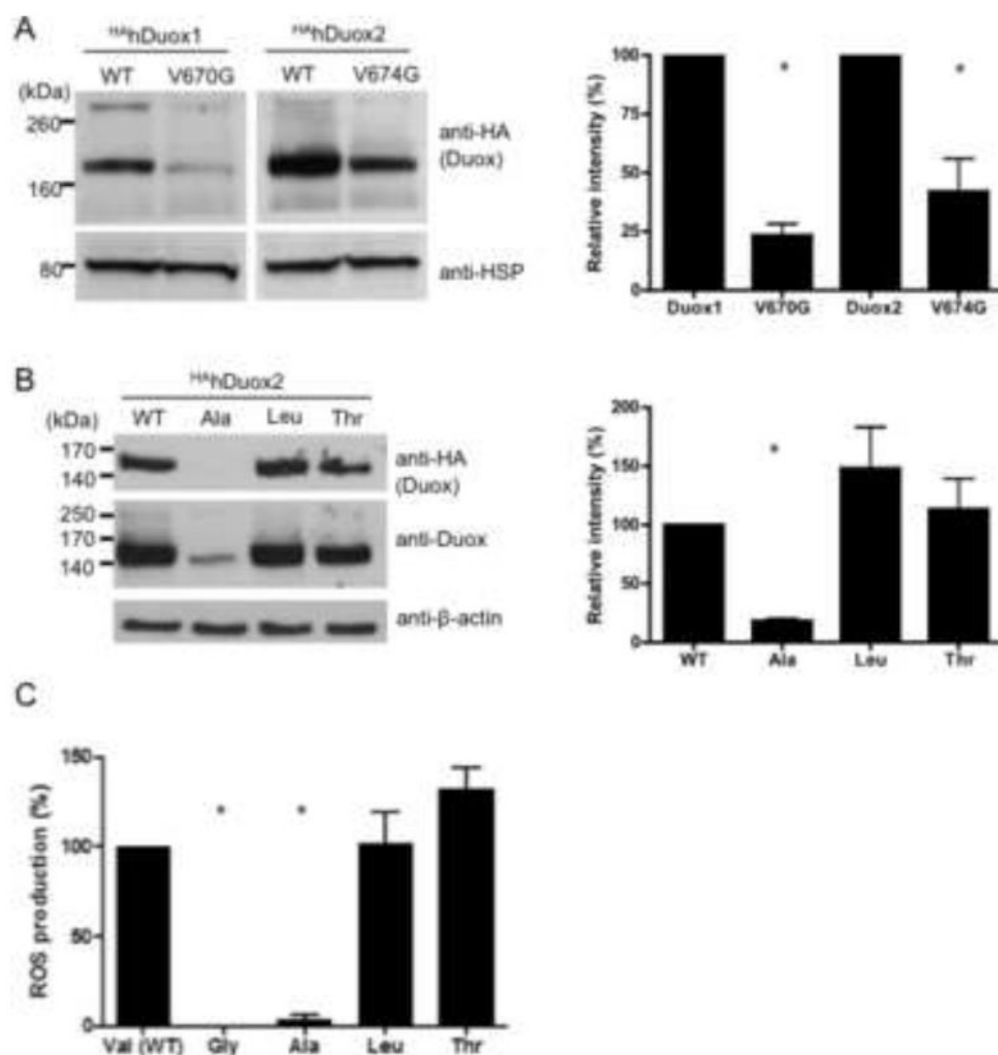


Figure 2. Western blot analysis of the valine→glycine mutant Duox proteins

(A) Western blot analysis of protein lysates (50 µg) extracted from stable ^{V5}DuoxA-expressing Flp-In 293 clones transiently transfected with HA-tagged hDuox cDNAs detects lower levels of valine→glycine Duox mutant (V670G DUOX1 and V674G Duox2) proteins in comparison to the corresponding wild type hDuox. Anti-HA (Covance) antibody was used at a 1:2000 dilution; as a loading control anti-HSP80 antibody was used in a 1:2000 dilution. (B) Western blot analysis of the valine 674 to alanine, leucine and threonine mutant ^{HA}hDuox2 proteins. Anti-Duox antibody was used in 1:1000, anti-beta-actin in 1:2500 dilutions. Ala: alanine, Leu: leucine, Thr: threonine mutants of valine 674 of human Duox2. Blots are representative; bar graphs (right) show the mean relative intensities + SEM of HA-Duox bands normalized to the loading control and expressed as percent of wild type Duox from 3 independent experiments. (C) Extracellular H₂O₂ producing activity of the different valine 674 substituted Duox2 mutant enzymes. Activities were measured as integrated RLU detected over 20 minutes after ionomycin stimulation from 3 independent experiments and then expressed as percentage of the wild type Duox2 H₂O₂ production.

Differences between groups were analyzed by ANOVA; $p < 0.05$ values were considered as statistically significant, indicated by asterisks.

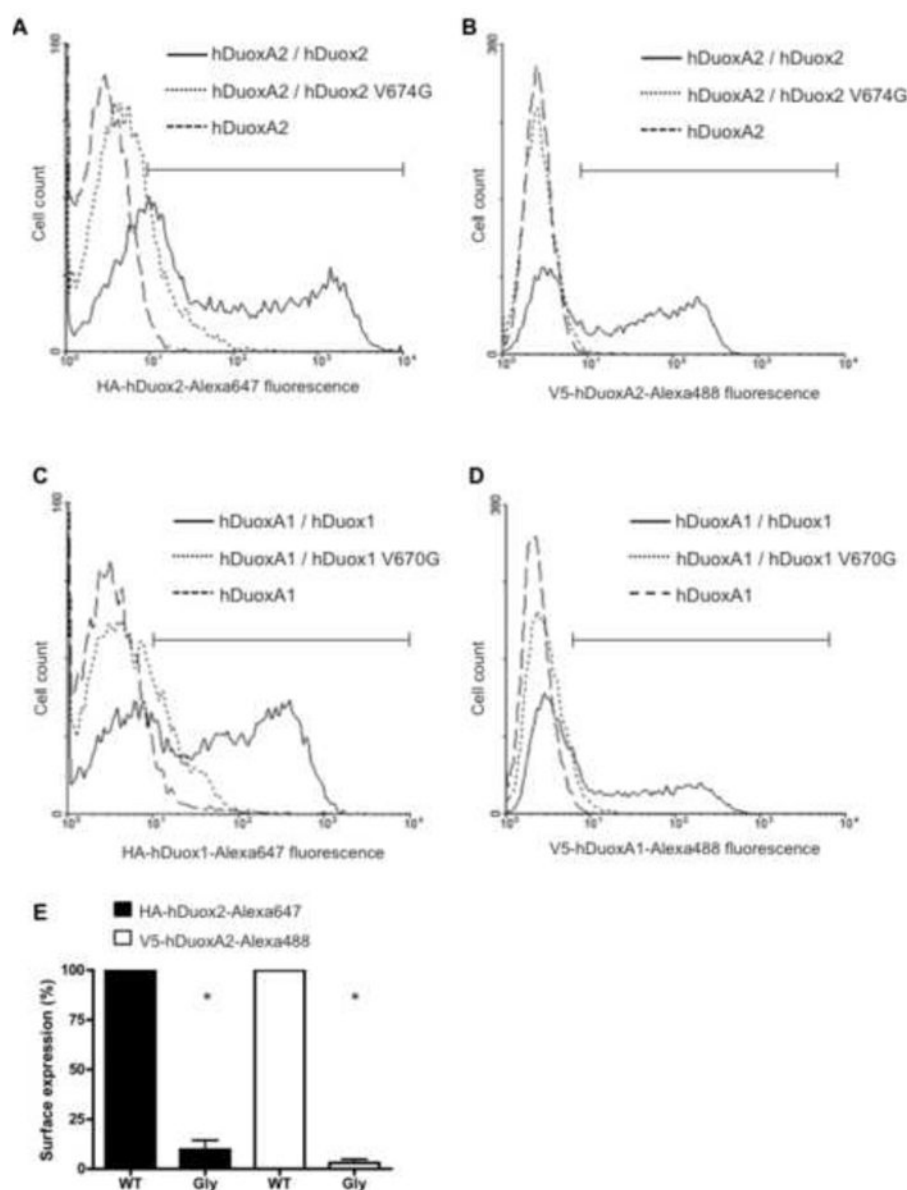


Figure 3. Analysis of cell surface expression of the valine→glycine HA hDuoX mutant proteins
Flow cytometric analysis of cell-surface-exposed HA hDuoX and V5 hDuoX proteins co-expressed in stable V5 hDuoX A Flp-In 293 cells (10,000 cell counts per assay). Cells were stain with mouse anti-HA IgG1 (1:100) or anti-V5 IgG2a (1:100) monoclonal antibodies and labeled with Alexa Fluor® 647 IgG1 or Alexa Fluor® 488 IgG2a secondary antibodies (1:1000), respectively.

(A) Compared to wild type HA hDuoX2 (solid line), the histogram of V674G HA hDuoX2 expressing cells (dotted line) shows considerably lower cell counts in the gated high fluorescence channels (bracketed horizontal bar) that excludes the stained negative control cell peak of Flp-In 293 cells stably expressing V5 hDuoX2 alone (broken line). (B) Histogram of V5-DuoX2 detected in V674G HA hDuoX2-transfected cells (dotted line) closely resembles the negative control cell peak, whereas a significant population of wild

type ^{HA}hDuox-transfected cells is detected with high cell surface V5-hDuoxA2 expression. Similar results of low cell surface detection of both Duox1 and DuoxA1α proteins were obtained with transfection of V670G ^{HA}hDuox1 mutant enzyme (C, D). C and D panels shows one representative of two independent experiments. (E) Normalized plasma membrane expression of wild type (WT) and V674G mutant (Gly) hDuox2-transfected cell populations calculated as percent of wild type hDuox2 from three independent transfection experiments. Analysis of hDuox2-transfected cell populations with fluorescence intensities greater than the peak of control DuoxA2 Flp-In 293 cells, as indicated by gating shown in panels A and B. Bars represents mean + SEM of the three experiments, with asterisks (*) considered statistically significant relative to WT with a $p < 0.05$ using one sample t-tests.

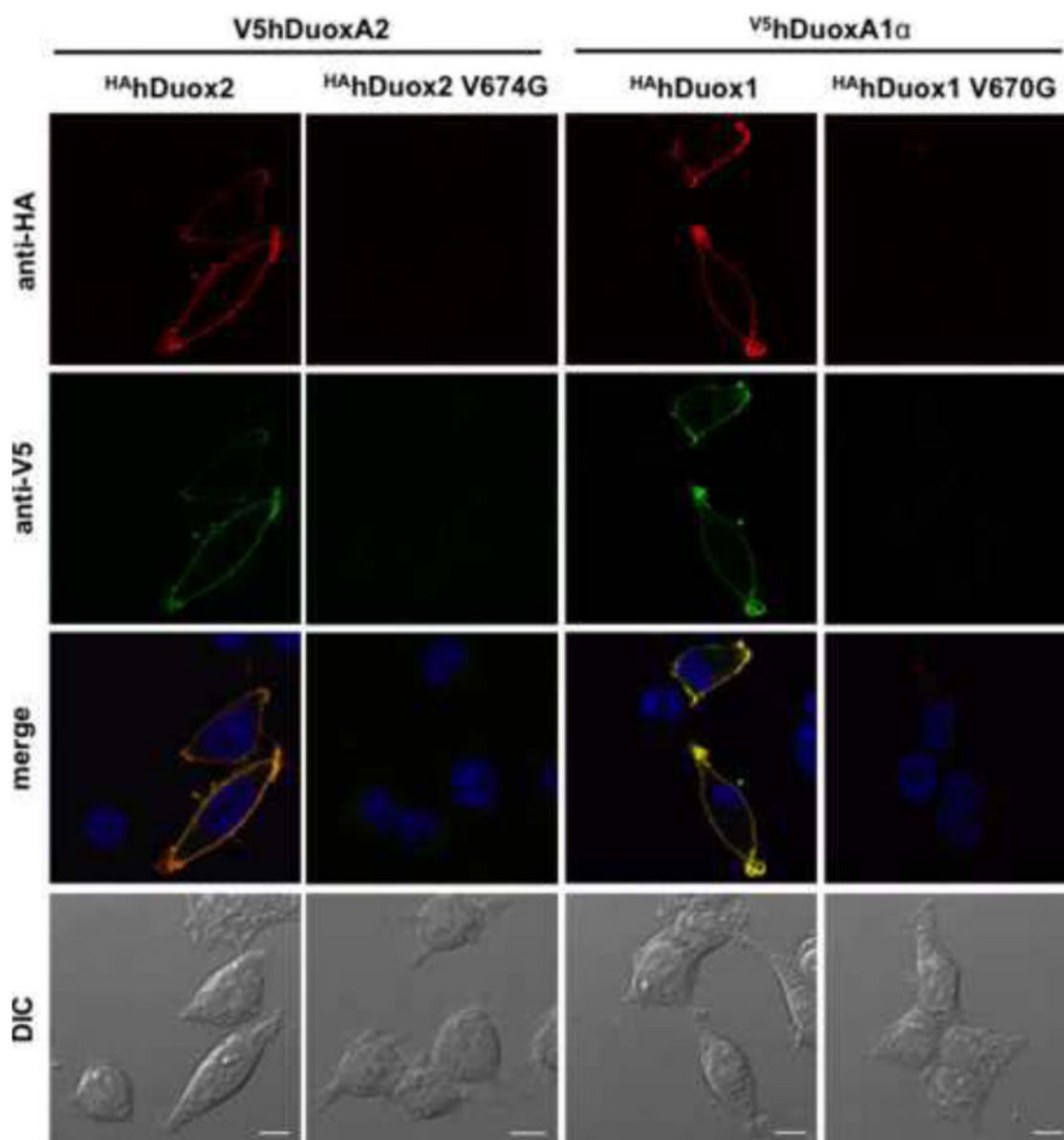


Figure 4. Valine→glycine mutation of $HAhDuox$ enzymes impairs cell surface detection of Duox and DuoxA proteins

Cell surface immunofluorescence staining of unpermeabilized $V5hDuoxA2$ or $V5hDuoxA1$ stable Flp-In 293 cells transiently transfected (48 h) with $HAhDuox$ coding vectors. In contrast to the wild type proteins, the $V674G$ $HAhDuox2$ and $V670G$ $HAhDuox1$ enzymes are not detected on the cell surface. Anti-HA (Covance) and anti-V5 (LifeTechnologies) antibodies were diluted at 1:100, goat anti-mouse Alexa Fluor® 647 and 488 secondary antibodies at 1:1000. Nuclei were counterstained with DAPI in 1:10000. Scale bars show 10 μm . Two other independent transfection experiments yielded similar results.

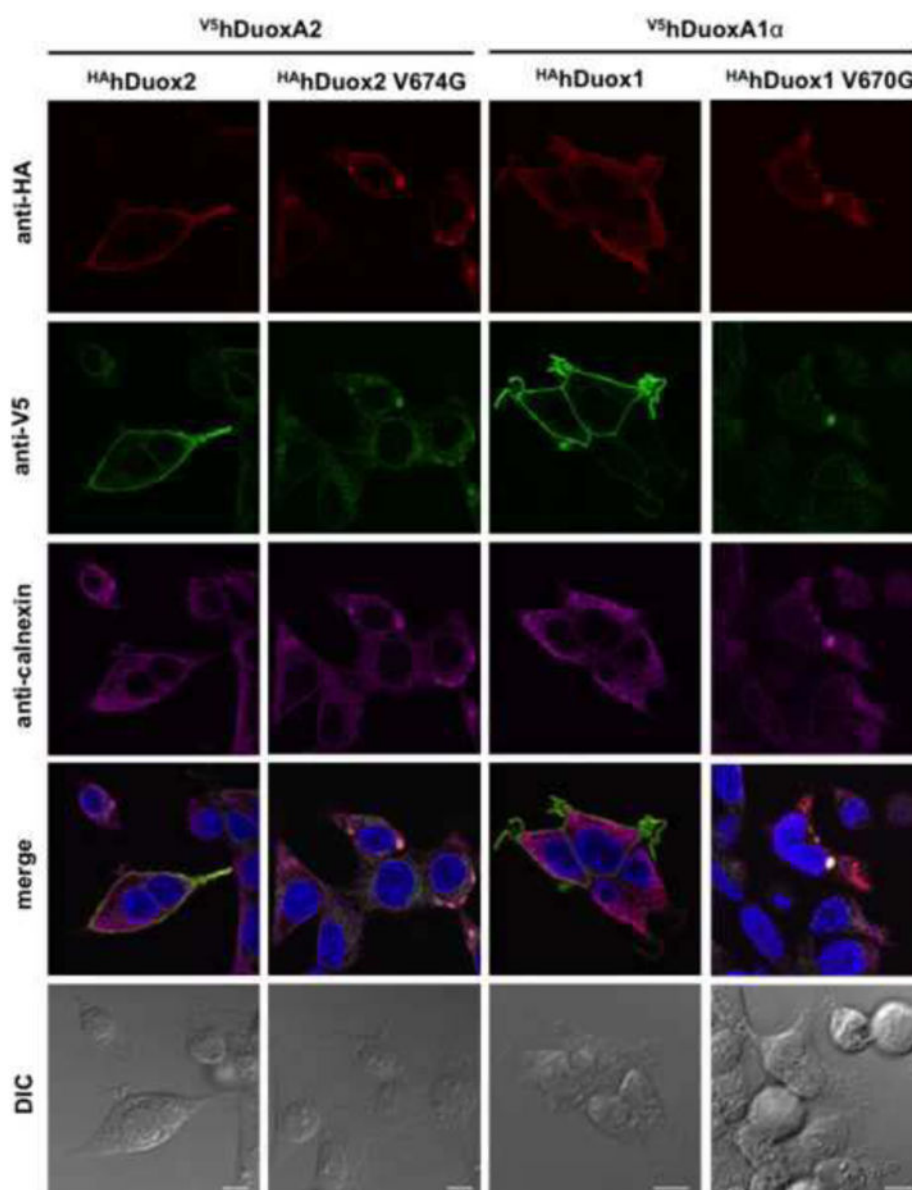


Figure 5. The valine→glycine mutant Duox enzymes colocalize with the endoplasmic reticulum protein calnexin

Immunofluorescence staining of permeabilized stable $V^5hDuoxA2$ - or $V^5hDuoxA1\alpha$ -expressing Flp-In 293 cells transiently transfected (48 h) with wild type or valine→glycine $HAhDuox$ mutant coding vectors. In contrast to wild type, the valine→glycine mutant Duox2 and DUOX1 are retained inside the cells with the activator, where they colocalize with the ER marker calnexin. Anti-HA (Covance) and anti-V5 (Life Technologies) antibodies were diluted 1:100 and anti-calnexin was 1:50. Goat anti-mouse Alexa Fluor® 647/594/488 secondary antibodies were applied at 1:1000 dilution. Nuclei were counterstained with DAPI in 1:10000. Scale bars represent 10 μm . Two other independent experiments gave similar results, showing only intracellular (ER) staining patterns in cells expressing mutant Duox proteins.

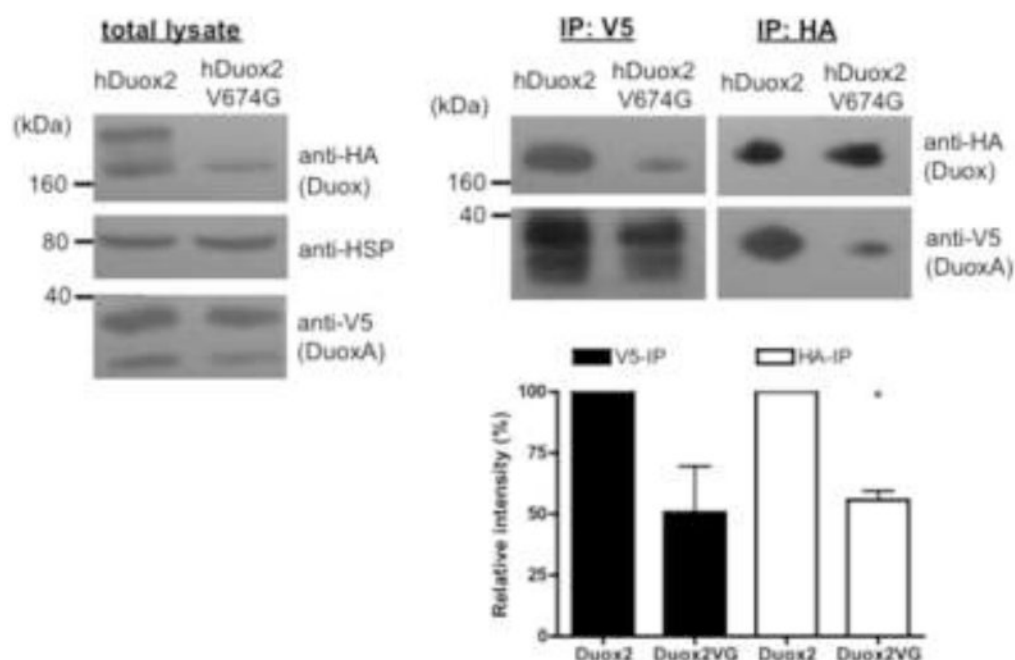


Figure 6. Valine→glycine mutant ^{HA}hDuox2 forms a complex with the ^{V5}hDuoxA2 maturation factor

^{HA}hDuox2 or V674G ^{HA}hDuox2 was transiently expressed (48 h) into stable ^{V5}hDuoxA2-expressing Flp-In 293 cells. 500 µg proteins of total cell lysates were immunoprecipitated with anti-HA (IP:HA) or anti-V5 (IP:V5) agarose for 30 min at 4°C. Western blot analysis of immunoprecipitated complexes shows that valine→glycine Duox2 forms a stable complex with the DuoxA2 maturation factor, although at lower levels than wild type Duox2. Anti-HA, anti-HSP80 and anti-V5 antibodies were used in 1:1000, 1:2000 and 1:5000 respectively. Blots show results of one representative experiment and bar graphs represent the mean relative intensities + SEM of V5- and HA-reactive bands detected in IP complexes normalized to the loading control and expressed as percent of the wild type from 3 independent experiments. P<0.05 was considered statistically significant (*).

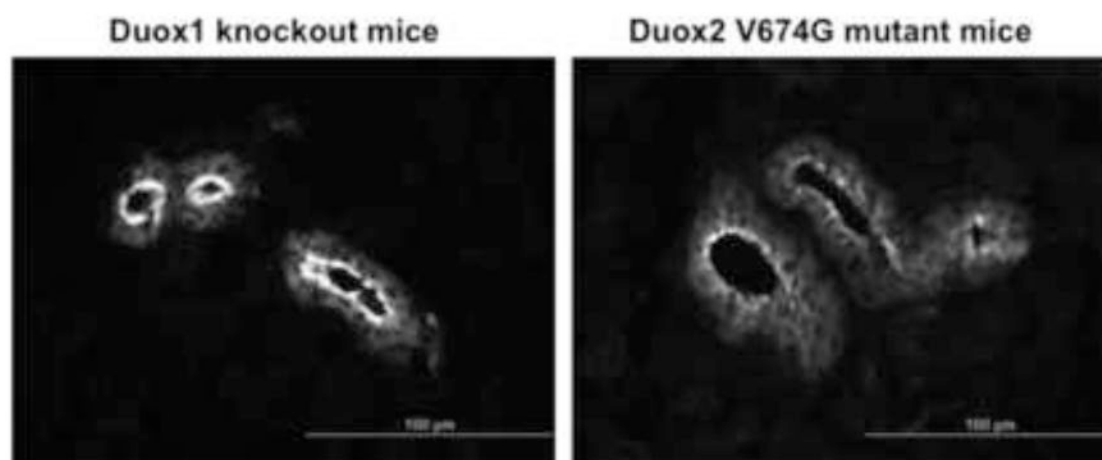


Figure 7. Immunofluorescence detection of the wild type and valine→glycine mutant Duox2 in mouse salivary gland frozen sections from Duox1 knockout and Duox2 mutant (B6(129)-Duox2^{thyd/thyd/J}) mice

Wild type Duox2 protein detected in Duox1 knockout mice is condensed along the apical plasma membrane of major duct epithelial cells (left), whereas the V674G mDuox2 mutant protein is less abundant and is detected in intracellular vesicles (right). Polyclonal anti-Duox antibodies were used at a 1:150 dilution and were detected with Alexa488-conjugated goat anti-rabbit Fab (Life Technologies, Carlsbad, CA, USA) used at a 1:1000 dilution.

Micrographs shown are representative of 3 three independent staining experiments obtaining similar results.

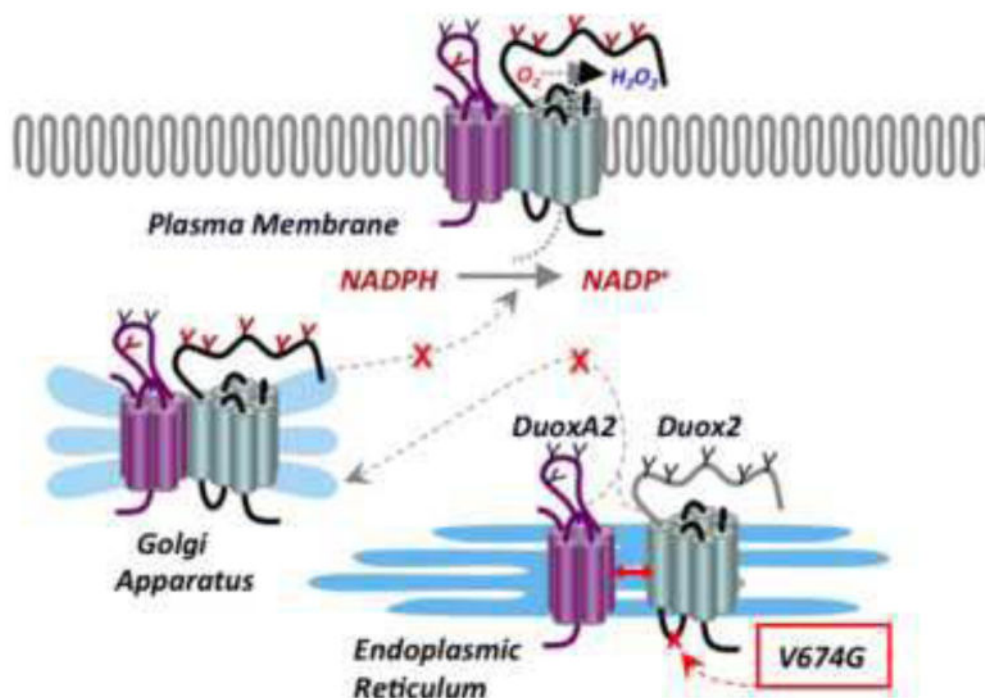


Figure 8. Mutation of conserved valine 674 results in a Duox and DuoxA translocation defect
 Mutation of valine 674 to glycine within the first intracellular loop of Duox2 results in a loss of ROS release from the plasma membrane. The mutant Duox2 forms a stable complex with its maturation factor DuoxA2, but is retained in the ER and rendered unstable.